

# Surface-temperature trends and variability in the low-latitude North Atlantic since 1552

Casey Saenger<sup>1\*</sup>, Anne L. Cohen<sup>2</sup>, Delia W. Oppo<sup>2</sup>, Robert B. Halley<sup>3</sup> and Jessica E. Carilli<sup>4</sup>

**Sea surface temperatures in the North Atlantic Ocean recorded since the 1900s have been ascribed to a natural multidecadal oscillation superimposed on a background warming trend<sup>1–6</sup>. It has been suggested that the multidecadal variability may be a persistent feature<sup>6–8</sup>, raising the possibility that the associated climate impacts may be predictable<sup>9</sup>. However, our understanding of the multidecadal ocean variability before the instrumental record is based on interpretations of terrestrial-based proxy records<sup>7,8</sup>. Here we present an absolutely dated and annually resolved record of sea surface temperature from the Bahamas, based on a 439-year time series of coral growth rates. The reconstruction indicates that temperatures were as warm as today from about 1552 to 1570, then cooled by about 1°C from 1650 to 1730 before warming until the present. Our estimates of background variability suggest that much of the warming since 1900 was driven by anthropogenic forcing. Interdecadal variability with a period of 15–25 years is superimposed on most of the record, but multidecadal variability becomes significant only after 1730. We conclude that the multidecadal variability in sea surface temperatures in the low-latitude western Atlantic Ocean is not persistent, potentially making accurate decadal climate forecasts more difficult to achieve.**

Fluctuations of North Atlantic sea surface temperature (SST) on decadal–multidecadal timescales can influence hemispheric temperature and precipitation patterns<sup>3,5</sup>, tropical Atlantic hurricane behaviour<sup>4,5</sup> and may mask or augment warming due to anthropogenic causes<sup>9</sup>. The multidecadal portion of this SST variability, commonly referred to as the Atlantic Multidecadal Oscillation (AMO), is thought to reflect, at least partially, natural internal variations in the Atlantic Meridional Overturning Circulation<sup>6,10,11</sup> (MOC). In contrast, the lower-frequency background component of SST variability is considered to be externally forced by variations in solar activity, volcanism, greenhouse gases and tropospheric aerosols<sup>2,12</sup>.

Model simulations<sup>5,6,10,11</sup> suggest that the AMO is a persistent mode of internal ocean variability, the climatic impacts of which may be predicted decades in advance once externally forced background SST variability is removed<sup>9</sup>. However, neither the AMO nor long-term changes in the background SST are well characterized in the brief (~150 year) observational record. Attempts to extend the instrumental record using proxy reconstructions have relied heavily on high-latitude tree-ring records<sup>7,8</sup>, but these non-marine proxies do not respond directly to SST variability and may have significant biases at centennial timescales<sup>13</sup>. So far, reconstructions of Atlantic SST variability based strictly on oceanographic proxies lack either the age control<sup>14–16</sup> or the length<sup>17–19</sup> needed to separate

the AMO from changes in externally forced background SST (see Supplementary Fig. S1).

Here we present the first continuous, absolutely dated and annually resolved proxy record of Atlantic SST spanning many centuries. Using computed axial tomography (CAT) imaging, we quantified temperature-dependent variations in the annual growth of a massive *Siderastrea siderea* coral collected from the Bahamas (25.84° N, 78.62° W) in 1991. We first established the growth–SST relationship for this coral over the full instrumental record (1857–1991), and then verified this calibration by applying it to an *S. siderea* colony from Belize (17.50° N, 87.76° W). Robust correlations between coral growth and SST in several other species<sup>17,18,20–22</sup> have yielded valuable palaeotemperature records<sup>17,20</sup>, but these techniques have not been applied to *S. siderea*. In this and previous studies<sup>20</sup>, CAT imaging is especially useful because unlike conventional two-dimensional X-ray techniques, three-dimensional CAT scans can be rotated electronically during data processing to ensure analyses are carried out along a coral's axis of maximum growth.

Greyscale analyses of CAT scan images revealed 439 (±1) annual high-density bands spanning 1552–1991 in the Bahamas coral and 66 bands spanning 1936–2001 in the Belize specimen (see Supplementary Fig. S2). We used the distance between successive high-density bands to calculate the annual upward growth of each coral. Annual growth rates, which ranged from 0.11 to 0.38 cm yr<sup>-1</sup> in the Bahamas coral and 0.19–0.36 cm yr<sup>-1</sup> in the Belize specimen, showed an inverse correlation with instrumental SST (Fig. 1a–c)<sup>23</sup>. Coral growth and observed annual average SST anomalies were significantly coherent (95%) at periods longer than ~6 years (see Supplementary Fig. S3). We calibrated coral growth rate anomalies against observed 1857–1991 Bahamas SST anomalies ( $r = -0.67$ ,  $p = 0.024$ ,  $N_{\text{effective}} = 25$ ; Fig. 1a, see the Methods section). SST explains 45% of the variance in coral growth on 6-year timescales, and 78% of the variance on multidecadal (>30 year) timescales ( $r = -0.88$ ,  $p < 0.001$ ,  $N_{\text{effective}} = 16$ ). Although it is well established that environmental parameters other than SST influence coral growth, we find SST to be the dominant forcing on the timescales of interest to this study, consistent with ref. 21. Furthermore, Belize SST anomalies reconstructed using our Bahamas coral calibration also correspond well with observations ( $r = 0.70$ ,  $p = 0.002$ ,  $N_{\text{effective}} = 36$ ), capturing both the timing and amplitude of major SST excursions (Fig. 1c)<sup>23</sup>.

Coral-based Bahamas SST anomalies show mild conditions from 1870–1900 and 1940–1960 separated by two decades of cooler SSTs from 1900–1920 (Fig. 1c). These multidecadal trends are significantly coherent (95%) with instrumental SST and the AMO index at periods longer than 6 years (Fig. 1d, see Supplementary Figs S3, S4). However, Bahamas SST anomalies did not cool markedly during the

<sup>1</sup>Massachusetts Institute of Technology and Woods Hole Oceanographic Institution Joint Program in Oceanography, Woods Hole, Massachusetts 02543, USA, <sup>2</sup>Department of Geology and Geophysics, Woods Hole Oceanographic Institution, Woods Hole, Massachusetts, USA, <sup>3</sup>US Geological Survey (retired) 13765 2600 Rd. Cedaredge, Colorado, USA, <sup>4</sup>University of California San Diego, Scripps Institute of Oceanography, La Jolla, California, USA.

\*e-mail: csaenger@mit.edu.

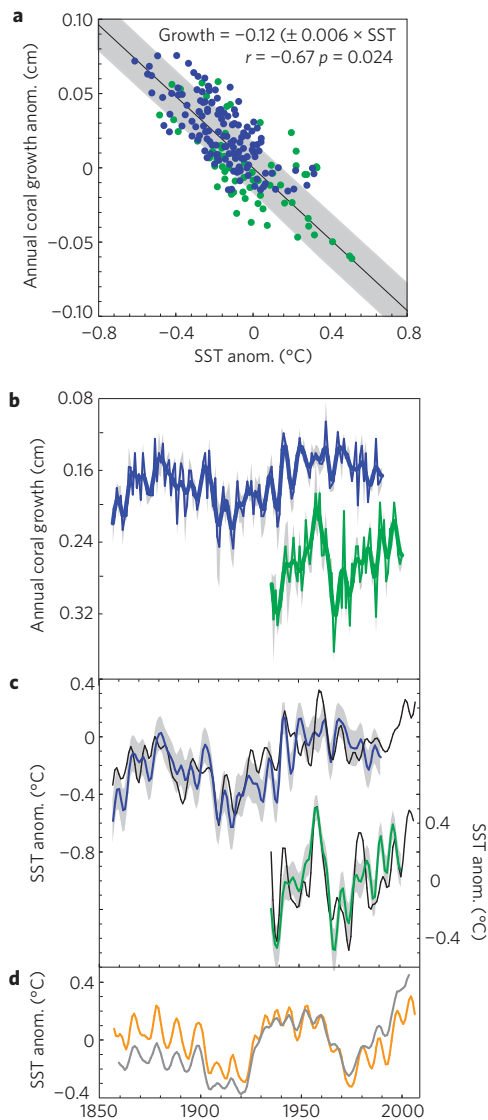


**Figure 1 | Calibration and verification of the coral-based SST proxy.**

**a**, 1857–1991 Bahamas SST anomalies<sup>23</sup> regressed against Bahamas coral growth anomalies (blue). Belize coral growth anomalies and their equivalent SST anomalies (green) do not contribute to the calibration. **b**, Annual unfiltered (fine) and filtered (bold) coral growth measured from CAT scans of Bahamas (blue) and Belize (green) specimens. **c**, Coral-based SST anomalies reconstructed from Bahamas (blue) and Belize (green) corals compared with observed 1857–2008 filtered instrumental SST anomalies (black). The shading in **a–c** indicates  $1\sigma$  standard error. **d**, The mean (grey) and linearly detrended mean (AMO; orange) SST anomaly from 0–75° N, 10–75° W.

1 recent negative AMO phase, indicating that regional-scale processes  
2 also influence low-latitude western Atlantic SST.

3 We applied our calibration to the entire record of Bahamas  
4 coral growth rate measurements to generate a continuous 439-year  
5 reconstruction of SST anomalies (Fig. 2a). Over this time period,  
6 which includes much of the Little Ice Age, Bahamas SST anomalies  
7 generally fluctuated within  $\sim 1^\circ\text{C}$  of the twentieth century mean.  
8 Our record suggests that SSTs were as warm as present from 1552  
9 to 1570, but cooled steadily throughout the seventeenth century.  
10 Maximum cooling occurred from 1650 to 1730, and was punctuated  
11 by especially cool periods near 1672, 1694 and 1729. An  $\sim 70$  year  
12 period of relatively stable warmth from  $\sim 1750$  to 1830 ended  
13 with two abrupt cooling events between 1830 and 1850. A general

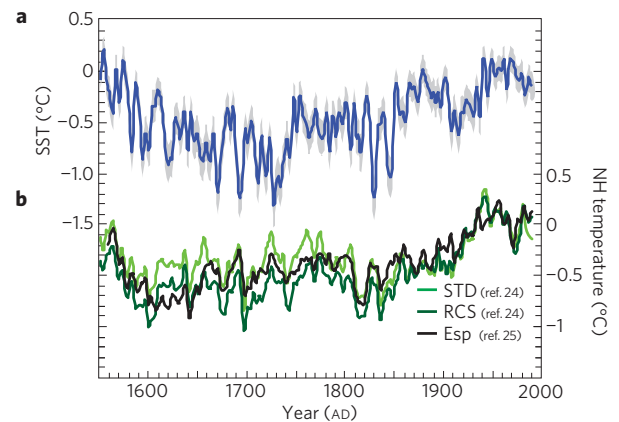


**Figure 2 | Northern Hemisphere and Atlantic temperature variability since 1550.**

**a**, Bahamas coral-based SST anomaly and  $1\sigma$  standard error (shading), estimated by applying the calibration in Fig. 1a to filtered annual coral growth rates (blue). **b**, Filtered hemispheric surface temperature anomalies from extratropical tree rings using regional curve standardization (RCS) and standard curve fitting (STD; refs 24, 25) methods.

warming trend after 1850 follows the instrumental record against  
14 which our SST reconstruction is calibrated.

15  
16 Low-frequency variability in our Bahamas coral-based SST  
17 reconstruction is similar to that observed in annually resolved  
18 extratropical tree-ring-based estimates of Northern Hemisphere  
19 temperature variability (Fig. 2b)<sup>24,25</sup>. The major features of these  
20 hemispheric temperature reconstructions can be explained by  
21 variations in solar radiation, volcanic eruptions and the combined  
22 anthropogenic influence of greenhouse gases and tropospheric  
23 aerosols<sup>12</sup>. The similarities with our Bahamas record suggest the  
24 same forcings also influence low-latitude western Atlantic SST. Of  
25 note are two abrupt cold episodes in our record near 1830 and 1850  
26 that occur  $\sim 15$  years after similar volcanically driven hemispheric  
27 cool events. Although this relatively long delay suggests hemispheric  
28 and Bahamas cool episodes are unlikely to be responses to common  
29 volcanic forcings, similar abrupt events in a coral Sr/Ca record from  
30 Bermuda (see Supplementary Fig. S1c) are nearly synchronous with  
31 our reconstruction, suggesting that the cold excursions we observe  
32 are real features of low-latitude western Atlantic variability.

33 We estimate the externally forced background signal in our SST  
34 reconstruction using a multiple regression approach. To estimate  
35 the influence of individual radiative forcings, we simultaneously  
36 regressed an energy balance model's temperature response to solar,  
37 volcanic and anthropogenic variability<sup>12</sup> against Bahamas  
38 SST (Fig. 3a). Significant uncertainties are associated with radiative  
39 forcing estimates<sup>26</sup> and with applying the multiple regression  
40 approach to our single proxy record. However, because Bahamas  
41 SST is strongly correlated with low-latitude SST in other regions  
42 (see Supplementary Fig. S5), we consider this method to provide  
43 a useful approximation of externally forced SST variability  
44 across a broad region.

45 The results of our multiple regression approach suggest  
46 externally forced SST cooled by  $\sim 0.2^\circ\text{C}$  from  $\sim 1552$  to 1600,  
47 remained cool from  $\sim 1600$  to 1800 and warmed by  $\sim 0.8^\circ\text{C}$  after  
48  $\sim 1800$  (Fig. 3a). This trend, which accounts for 35% of the variance  
49 in our Bahamas SST reconstruction, is similar to lower-resolution  
50 SST reconstructions in the region that suggest a  $\sim 1^\circ\text{C}$  cooling  
51 from  $\sim 1600$  to 1700 was the largest SST anomaly of the past few  
52 centuries<sup>15,16</sup>. Although it has been speculated that this cooling may  
53 reflect an oceanic response to reduced solar activity, a robust link  
54 has not been established owing to the relatively large chronological  
55 uncertainties inherent in lower-resolution sedimentary records<sup>15</sup>.  
56 Using our absolutely dated record, we could not distinguish the

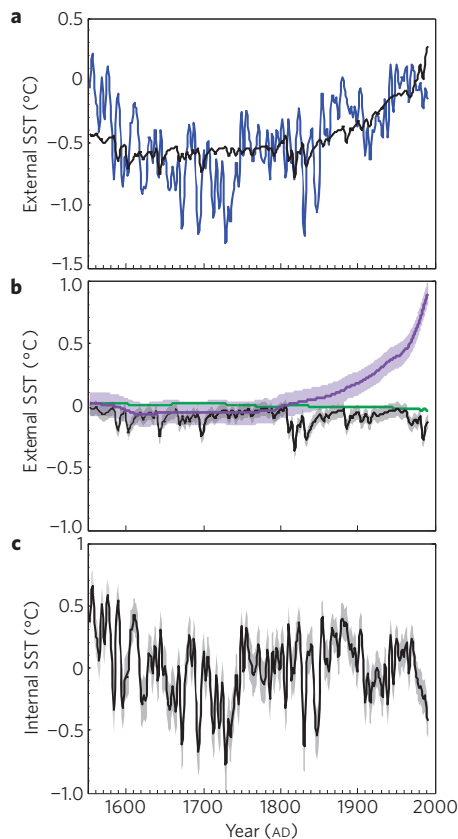


**Figure 3 | Externally and internally forced SST variability** **a**, Coral-based SST anomalies (blue) and estimated externally forced SST anomalies (black). **b**, SST variability and  $1\sigma$  standard error attributed to volcanic (black), solar (green) and anthropogenic (purple) external forcings (see the Methods section). **c**, Internal SST variability (grey) and standard error ( $1\sigma$ ) calculated by subtracting the curves in **a**.

1 effect of solar forcing from natural internal ocean variability,  
2 suggesting that it may not have been a dominant SST forcing on  
3 these timescales (Fig. 3b, c). In contrast, we did detect a significant  
4 SST response to volcanic and anthropogenic signals, the latter  
5 of which accounts for most of the warming in our coral-based  
6 SST record since  $\sim 1900$ .

7 Internal SST variations show clear multidecadal oscillations, but  
8 only back to  $\sim 1730$  (Fig. 3c). In addition to the two AMO cycles  
9 inferred from the instrumental record, a third multidecadal cycle  
10 occurs from  $\sim 1740$  to 1840 that is consistent with proxy evidence  
11 suggesting the AMO predates the instrumental record<sup>7,8</sup>. However,  
12 the longer period (100 years) and extended warm phase (70 years) of  
13 this extra cycle suggests that any multidecadal low-latitude western  
14 Atlantic SST variability is at best quasi-periodic. Before  $\sim 1730$ ,  
15 there is little evidence for extra AMO-like oscillations, implying that  
16 multidecadal variability may not have been a persistent feature of  
17 low-latitude western Atlantic SST.

18 To characterize changes in the dominant periodicities of internal  
19 SST variability, we carried out multitaper method spectral analysis<sup>27</sup>  
20 in six overlapping  $\sim 200$ -year bins (Fig. 4). Bins centred on 1800,  
21 1850 and 1900 show significant (90%) multidecadal power similar  
22 to the AMO, whereas no significant multidecadal power is evident  
23 in bins centred on 1650, 1700 and 1750. Although the absence  
24 of multidecadal variability before  $\sim 1730$  may be caused by the  
25 same processes responsible for the recent divergence of observed  
26 Bahamas SST from the AMO (Fig. 1c, d), it may also reflect broad  
27 changes in multidecadal Atlantic SST variability. To the degree to  
28 which our record represents the larger North Atlantic, it suggests

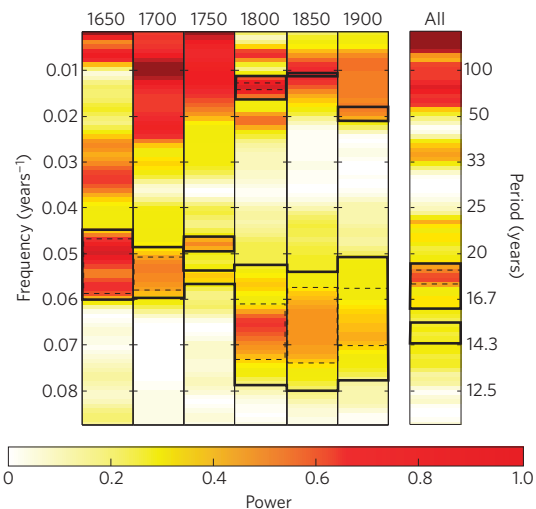


**Figure 4 | Spectral analysis of internal SST variability.** Spectral signature of internally driven SST variability from Fig. 3c. Spectra were calculated using the multitaper method<sup>27</sup> for the entire record (All) and in  $\sim 200$ -year bins spanning the periods 1552–1750, 1600–1800, 1650–1850, 1700–1900, 1750–1950 and 1800–1991. The centre year of each bin is shown (top). Gradients indicate the relative power at a given frequency (left y axis) and period (right y axis). Bounding boxes identify frequencies with significant power above red noise at 90% (bold) and 95% (dashed) confidence levels.

that if the AMO is a natural mode of internal ocean variability,  
it may be less persistent than previously suggested<sup>6–8</sup>. In contrast,  
interdecadal (15–25 year) internal variability is significant ( $>90\%$ )  
throughout our record, hinting that variations on these timescales  
may be a more persistent feature of Atlantic SST.

Control runs of the HadCM3 coupled ocean–atmosphere global  
climate model show natural interdecadal to multidecadal MOC  
oscillations that may help explain the variability in our recon-  
structed SST. In the model, multidecadal oscillations are part of a  
coupled ocean–atmosphere process in which phase reversals rely on  
oceanic transport of density anomalies<sup>10</sup>. The model's interdecadal  
variability is not coupled however, but rather seems to arise from  
atmospherically driven oscillations of salt and heat advection into  
the subtropical Atlantic and Arctic oceans<sup>11</sup>. If the mechanisms of  
HadCM3 are accurate, the absence of multidecadal variability in  
the earliest centuries of our record may be related to a 15–25%  
reduction in northward Gulf Stream transport before  $\sim 1750$   
(ref. 28) and with a possible weakening of the MOC. We speculate  
that such a reduction may have diminished the effectiveness of  
the negative feedback responsible for multidecadal oscillations by  
increasing the time needed to transport low-latitude ocean density  
anomalies from the tropics to the subtropical Atlantic. The persistent  
interdecadal power in our record suggests that the atmospheric  
forcing potentially responsible for 15–25 year SST variability was  
not significantly changed by the weaker MOC. However, the mech-  
anisms responsible for interdecadal–multidecadal SST oscillations  
remain poorly understood<sup>29</sup>, and a link with multicentennial MOC  
vigour must be considered to be one of many possible explanations  
for the apparent lack of multidecadal variability before  $\sim 1730$ .

## Methods

**CAT scanning.** A 9-cm-diameter coral core was split lengthwise, and one half was imaged using a Siemens Volume Zoom Spiral Computerized Tomography Scanner at the Woods Hole Oceanographic Institution. A 0.8-cm-thick by 5-cm-wide coral slab from Belize was scanned using the same method. Scans were conducted at 400 mA s and 120 kV using a 0.5 mm slice that was reconstructed at 0.2 mm. Siemens CT and eFilm software were used to identify the plane orthogonal to the coral's axis of maximum growth. We used ImageJ software to measure greyscale variations in a 10-pixel-wide transect along parallel corallites in each image (see Supplementary

Fig. S2). The lightest value of each sinusoidal annual cycle represented the location of each high-density band. The annual extension rate of each corallite was averaged for each year and is reported as a mean and standard error ( $1\sigma$ ). Coral high-density band formation typically occurs during maximum SST and we assume annual extension represents growth between successive Augusts. Thus, data represents September (year  $-1$ ) to August (year 0) of the date plotted.

**Filtering.** A second-order Butterworth low-pass filter with a cutoff frequency equivalent to 6 years was used to generate filtered data. This cutoff frequency was chosen on the basis of the coherence between coral extension and instrumental SST (see Supplementary Fig. S3).

**Calibration and verification.** Six-year filtered annual SST anomalies<sup>23</sup> in the  $5^\circ \times 5^\circ$  gridbox centred on  $22.5^\circ$  N,  $77.5^\circ$  W were regressed against similarly filtered Bahamas coral growth rate anomalies for the period 1857–1991 and forced through the origin (Fig. 1a). Anomalies were calculated relative to the 1951–1980 mean, consistent with ref. 23. The effective number of samples in filtered data ( $N_{\text{effective}}$ ) was estimated following the method of ref. 30 (pp. 261–263). Other reasonable choices for the filter cutoff frequency had a small influence on the calibration slope and do not affect our results with respect to frequency. A calibration based on SSTs in an adjacent  $5^\circ \times 5^\circ$  gridbox centred on  $27.5^\circ$  N,  $77.5^\circ$  W yielded nearly identical results. Estimates of Belize SST anomalies were calculated by applying the calibration regression to 6-year filtered Belize coral growth anomalies. Statistical correlations of coral-based Belize SST anomalies are based on regression against 6-year filtered annual SST anomalies<sup>23</sup> in the  $5^\circ \times 5^\circ$  gridbox centred on  $17.5^\circ$  N,  $87.5^\circ$  W.

**Detection and attribution.** Six-year filtered solar, volcanic and the sum of greenhouse gas and tropospheric aerosol radiative forcings (anthropogenic)<sup>12</sup> were simultaneously regressed against 6-year filtered coral-based Bahamas SST anomalies. Best-fit regression coefficients were multiplied by the original radiative forcings to estimate the SST contribution from solar, volcanic and anthropogenic influences (Fig. 3b).

The standard error ( $1\sigma$ ) of each forcing's SST response was estimated using a Monte Carlo approach. Each year of our coral-based SST reconstruction was randomly sampled from its probability distribution. This was repeated 1,000 times to generate 1,000 SST estimates, each 440 years long. SST estimates were regressed against radiative forcings following the method above to estimate three series of SST responses to solar, volcanic and anthropogenic variability. Standard errors ( $1\sigma$ ) were then calculated from these three series after accounting for reduced degrees of freedom<sup>30</sup>.

The best estimate of externally forced SST was subtracted from the full Bahamas SST record (Fig. 3a) to estimate internal SST variability (Fig. 3c). We considered external signals (Fig. 3b) that were significantly different from internal variability at 95% based on a one-tailed  $t$ -test to be detectable.

**Spectral analysis.** The multitaper method ( $p = 2$ ,  $K = 2$ ; ref. 27) was applied to our estimate of internal SST variability (Fig. 3c) over the frequency range from 0 to  $0.15$  cycles  $\text{yr}^{-1}$ . Confidence levels were determined relative to a red noise AR(1) background.

Received 31 October 2008; accepted 21 May 2009;  
published online XX Month XXXX

## References

- Schlesinger, M. E. & Ramankutty, N. An oscillation in the global climate system of period 65–70 years. *Nature* **367**, 723–726 (1994).
- Andronova, N. G. & Schelsinger, M. E. Causes of global temperature changes during the 19th and 20th centuries. *Geophys. Res. Lett.* **27**, 2137–2140 (2000).
- Enfield, D. B., Mestas-Nuñez, A. M. & Trimble, P. J. The Atlantic Multidecadal Oscillation and its relation to rainfall and river flows in the continental US. *Geophys. Res. Lett.* **28**, 2077–2080 (2001).
- Goldenberg, S. B., Landsea, C. W., Mestas-Nuñez, A. M. & Gray, W. M. The recent increase in Atlantic hurricane activity: Causes and implications. *Science* **293**, 474–479 (2001).
- Knight, J. R., Folland, C. K. & Scaife, A. A. Climate impacts of the Atlantic Multidecadal Oscillation. *Geophys. Res. Lett.* **33**, doi:10.1029/2006GL026242 (2006).
- Knight, J. R., Allan, R. J., Folland, C. K., Vellinga, M. & Mann, M. E. A signature of persistent natural thermohaline circulation cycles in observed climate. *Geophys. Res. Lett.* **32**, doi:10.1029/2005GL024233 (2005).
- Delworth, T. L. & Mann, M. E. Observed and simulated multidecadal variability in the Northern Hemisphere. *Clim. Dyn.* **16**, 661–676 (2000).
- Gray, S. T., Graumlich, L. J., Betancourt, J. L. & Pederson, G. T. A tree-ring based reconstruction of the Atlantic Multidecadal Oscillation since 1567 AD. *Geophys. Res. Lett.* **31**, doi:10.1029/2004GL019932 (2004).
- Latif, M., Collins, M., Pohlmann, H. & Keenlyside, N. A review of predictability studies of Atlantic sector climate on decadal timescales. *J. Clim.* **19**, 5971–5987 (2006).

- Vellinga, M. & Wu, P. L. Low-latitude freshwater influence on centennial variability of the Atlantic thermohaline circulation. *J. Clim.* **17**, 4498–4511 (2004).
- Dong, B. W. & Sutton, R. T. Mechanism of interdecadal thermohaline circulation variability in a coupled ocean-atmosphere GCM. *J. Clim.* **18**, 1117–1135 (2005).
- Hegerl, G. C. *et al.* Detection of human influence on a new, validated 1500-year temperature reconstruction. *J. Clim.* **20**, 650–666 (2007).
- D'Arrigo, R. D., Wilson, R., Liepert, B. & Cherubini, P. On the 'divergence problem' in northern forests: A review of the tree-ring evidence and possible causes. *Glob. Planet. Change* **60**, 289–295 (2008).
- Haase-Schramm, A. *et al.* Sr/Ca ratios and oxygen isotopes from sclerosponges: Temperature history of the Caribbean mixed layer and thermocline during the Little Ice Age. *Paleoceanography* **18**, doi:10.1029/2002PA000830 (2003).
- Lund, D. C. & Curry, W. Florida Current surface temperature and salinity variability during the last millennium. *Paleoceanography* **21**, doi:10.1029/2005PA0011218 (2006).
- Black, *et al.* An 8-century tropical Atlantic SST record from the Cariaco Basin. *Paleoceanography* **22**, doi:10.1029/2007PA001427 (2007).
- Slowey, N. C. & Crowley, T. J. Interdecadal variability of northern hemisphere circulation recorded by Gulf of Mexico corals. *Geophys. Res. Lett.* **22**, 2345–2348 (1995).
- Crueger, T., Kuhnert, H., Pätzold, J. & Zorita, E. Calibrations of Bermuda corals against large-scale sea surface temperature and sea level pressure pattern time series and implications for climate reconstructions. *J. Geophys. Res.* **111**, doi:10.1029/2005JD006903 (2006).
- Goodkin, N. F., Huguen, K. A., Curry, W. B., Doney, S. C. & Ostermann, D. R. Sea surface temperature and salinity variability at Bermuda during the end of the Little Ice Age. *Paleoceanography* **23**, doi:10.1029/2007PA001532 (2008).
- Bessat, F. & Buigues, D. Two centuries of variation in coral growth in a massive *Porites* colony from Moorea (French Polynesia): A response of ocean-atmosphere variability from south central Pacific. *Palaeogeogr. Palaeoclimatol. Palaeoecol.* **175**, 381–392 (2001).
- Lough, J. M. & Barnes, D. J. Environmental controls on growth of the massive coral *Porites*. *J. Exp. Mar. Biol. Ecol.* **245**, 225–243 (2000).
- Carricart-Ganivet, J. P. Sea surface temperature and the growth of the West Atlantic reef-building coral *Montastrea annularis*. *J. Exp. Mar. Biol. Ecol.* **302**, 249–260 (2004).
- Kaplan, A. *et al.* Analyses of global sea surface temperature 1856–1991. *Geophys. Res. Lett.* **103**, 18567–18589 (1998).
- Esper, J., Cook, E. R. & Schweingruber, F. H. Low-frequency signals in long tree-ring chronologies for reconstructing past temperature variability. *Science* **295**, 2250–2253 (2002).
- D'Arrigo, R., Wilson, R. & Jacoby, G. On the long-term context for late twentieth century warming. *J. Geophys. Res.* **111**, doi:10.1029/2005JD006352 (2006).
- Ammann, C. M., Joos, F., Schimel, D. S., Otto-Bliesner, B. L. & Tomas, R. A. Solar influence on climate during the past millennium: Results from transient simulations with NCAR Climate System Model. *Proc. Natl Acad. Sci.* **104**, 3713–3718 (2007).
- Ghil, M. *et al.* Advanced spectral methods for climatic time series. *Rev. Geophys.* **40**, 3.1–3.41 (2002).
- Lund, D. C., Lynch-Stieglitz, J. & Curry, W. B. Gulf Stream density structure and transport during the past millennium. *Nature* **444**, 601–604 (2006).
- Delworth, T. L., Zhang, R. & Mann, M. E. in *Ocean Circulation: Mechanisms and Impacts* (eds Schmittner, A., Chiang, J. C. H. & Hemming, S. R.) 131–148 (American Geophysical Union, 2007).
- Emery, W. J. & Thompson, R. E. *Data Analysis Methods in Physical Oceanography* (Elsevier, 1998).

## Acknowledgements

We thank T. Crowley, P. Huybers, P. Chang, Y. Kwon, J. Woodruff, J. T. Farrar, N. Goodkin and G. Hegerl for discussion. We also thank D. Ketten and J. Arruda for CAT scan support and R. Pettit for initial growth measurements. This work was supported by the US National Science Foundation, WHOI's Ocean and Climate Change Institute, WHOI's Ocean Life Institute and the Inter-American Institute for Global Change Research.

## Author contributions

C.S., A.L.C. and D.W.O. designed the experiment. C.S. collected and analysed the data, and wrote the paper. C.S., A.L.C. and D.W.O. interpreted the data, discussed their implications and contributed to the manuscript. R.B.H. and J.E.C. provided sample material and manuscript comments.

## Additional information

Supplementary information accompanies this paper on [www.nature.com/naturegeoscience](http://www.nature.com/naturegeoscience). Reprints and permissions information is available online at <http://npg.nature.com/reprintsandpermissions>. Correspondence and requests for materials should be addressed to C.S.

## **Page 1**

---

*Query 1: Line no. 1*

Author: Please provide post code for affiliations 2–4.

*Query 2: Line no. 1*

Author: Please note that the first paragraph has been edited according to style.

## **Page 3**

---

*Query 3: Line no. 1*

Author: Please provide text, to be added to the caption, to define the black line in figure 3c's caption.

## **Page 4**

---

*Query 4: Line no. 92*

Author: Please provide initial for the author name in ref. 16.